

# Characterization and Validation of a-Si Magnetron-Sputtered Thin Films as Solid He Targets with High Stability for Nuclear Reactions

Vanda Godinho,<sup>\*,†,‡</sup> Francisco Javier Ferrer,<sup>\*,‡</sup> Begoña Fernández,<sup>‡</sup> Jaime Caballero-Hernández,<sup>†</sup> Joaquin Gómez-Camacho,<sup>‡,§</sup> and Asunción Fernández<sup>\*,†,‡</sup>

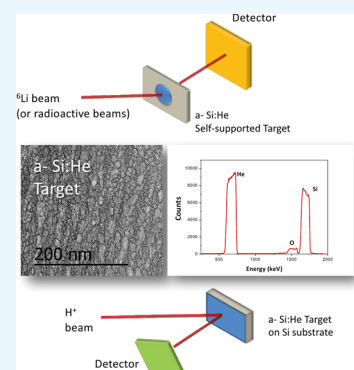
<sup>†</sup>Instituto de Ciencia de Materiales, CSIC – Universidad de Sevilla, Av. Américo Vespucio 49, 41092 Sevilla, Spain

<sup>‡</sup>Centro Nacional de Aceleradores, Universidad de Sevilla – CSIC – Junta de Andalucía, Av. Thomas A. Edison 7, 41092 Sevilla, Spain

<sup>§</sup>Departamento de Física Atómica, Molecular y Nuclear, Universidad de Sevilla, 41080 Sevilla, Spain

## S Supporting Information

**ABSTRACT:** In this work, we present our magnetron sputtering based methodology to produce amorphous silicon coatings with closed porosity, as a strategy to fabricate solid helium targets, in the form of supported or self-supported thin films, for nuclear reactions. We show how by changing the He working pressure it is possible to obtain highly porous homogeneous structures incorporating different He amounts. These porous coatings (a-Si:He) are very reproducible from run to run, and the high He amount incorporated makes them excellent candidates for solid He targets. The possibility of producing self-supported films is illustrated here, and its potential use in inverse kinematics experiments with radioactive beams is shown through the dispersion in forward geometry of a stable  $^6\text{Li}$  beam. Also the elastic scattering cross-sections for proton from helium were determined using an a-Si:He coating. The results agree well with the ones reported in the literature. These two examples validate our coatings as good candidates to be used as solid He targets in nuclear reactions. The stability of He inside the coatings, fundamental for its use as solid He targets, was investigated, both over time and after irradiation. The coatings proved to be very stable, and the amount of He inside the pores remains unaltered at least 2 years after deposition and after high irradiation fluence ( $5 \times 10^{17}$  particles/cm<sup>2</sup>; with a dose rate of  $5 \times 10^{12}$  particles/(cm<sup>2</sup> s)).



## INTRODUCTION

Nanostructured thin films and surfaces obtained by low-energy helium plasma treatments or by He incorporation via magnetron sputtering have been paid attention as strategies to modify and optimize materials properties.<sup>1–4</sup> Irradiation of metals with light ions, and in particular He, has been a subject of study for many years due to its technological interest in nuclear reactor materials.<sup>5–7</sup> Helium has been reported to be insoluble in different metals and tends to accumulate forming small bubbles causing damage in nuclear reactors.<sup>7</sup> Also considerable interest was found in the use of these materials for microelectronics, where the cavities produced by the implanted He act as impurity getters,<sup>8,9</sup> or more recently in energy conversion or storage devices.<sup>2,4,10</sup>

As an alternative route to top-down methods for producing porous materials, we have recently proposed a bottom-up methodology to grow porous silicon-based coatings, with closed porosity by magnetron sputtering.<sup>11–13</sup> The approach is a very versatile methodology based on magnetron sputtering technology, and thus extensible to a wide variety of materials and substrates, which in the presence of He plasmas allows the deposition of porous coatings with a decreased refractive index.<sup>12,14</sup> These highly porous coatings incorporate high He amounts (up to 40 atom %) inside the closed pores evenly

distributed throughout the film thickness.<sup>14,15</sup> The high He density stored could be very appealing for applications in nuclear physics or nuclear astrophysics, where light particle targets are of key importance in the spectroscopic and nuclear structure studies of unstable nuclei or even more fundamental studies of accurate elastic scattering cross-section determination for elemental analysis of these light elements.

Recent experiments with radioactive beams offer the opportunity to extend basic knowledge about nuclear structures of nuclei far from the stability line (“exotic” nuclei). It is not feasible to produce a radioactive target for irradiation due to the very short half-life of these nuclei. Experiments of inverse kinematics, where the desired radioactive beams are produced and investigated through interactions with a stable target, are the solution to that problem. Single nucleon stripping and pickup reactions with He and H isotopes provide fundamental structural information, in particular spectroscopic factors. Moreover, reactions involving elastic scattering and neutron transfer are also of interest in this matter. In addition, the

**Received:** September 27, 2016

**Accepted:** November 22, 2016

**Published:** December 14, 2016

Table 1. Deposition Conditions of the a-Si:He Coatings<sup>a</sup>

coating <sup>b</sup>	He pressure (Pa)	deposition rate (nm/min) <sup>c</sup>	areal density <sup>d</sup> ( $\times 10^{15}$ atoms/cm <sup>2</sup> )	He/Si <sup>d</sup>
a-Si:He_LP	2.7	13.6	7930 $\pm$ 550	0.79 $\pm$ 0.05
a-Si:He_MP	4.9	17.0	11000 $\pm$ 770	0.49 $\pm$ 0.05
a-Si:He_HP	9.0	14.3	8500 $\pm$ 600	0.39 $\pm$ 0.05

<sup>a</sup>Deposition rate from scanning electron microscopy (SEM) cross-sections, areal density, and He/Si atomic ratio from p-EBS. <sup>b</sup>Deposited at 150 W rf power. <sup>c</sup>From thickness results measured by SEM cross-sections. <sup>d</sup>From p-EBS.

interaction of stable beams with He targets is also of interest, as is explained further in this introduction.

Over the years different possibilities have been investigated for the use of stable hydrogen or helium in the form of gas or solid targets facing, however, some experimental challenges. Static gas targets, consisting of gas chambers, limit the accessible angular range due to their geometry, and the windows of the gas cell interfere with the beam losing energy and therefore introducing background reactions.<sup>16,17</sup> Windowless gas targets do not present the above-mentioned problems; however, there is a strong limitation in helium thickness (i.e., atoms/cm<sup>2</sup>), and expensive pumping stations are required to maintain the necessary pressure.<sup>17</sup>

To overcome this problem, an elegant solution was found for hydrogen targets in the form of polymers as polypropylene or polyethylene.<sup>18</sup> However, in the case of reactions involving radioactive beams and He, as He does not form any chemical compounds, other solutions must be explored. The major requirements for a solid He target to be used in nuclear reactions are high He concentration (especially in the case of interaction with exotic nuclei that have very low beam current) and homogeneity versus depth, as well as high stability of the bulk He concentration versus time.<sup>19</sup> <sup>4</sup>He-implanted target foils were proposed,<sup>16,20</sup> but apart from being expensive, reproducible results satisfying the demand for uniform distribution and concentrations are not easily achieved from sample to sample and thus not suitable for extended target production.<sup>21</sup> In this work, we show how our magnetron-sputtered silicon coatings could be promising and versatile candidates to be used as He solid targets for nuclear reactions. In a previous work,<sup>15</sup> we have investigated the physical parameters (density and pressure) of He inside the closed pores of magnetron-sputtered amorphous silicon coatings in depth. The work<sup>15</sup> demonstrated how the prepared coatings presented high density of homogeneously distributed pores filled with helium in a condensed state. Moreover, our approach provides reproducible coatings of a wide range of controlled thicknesses, with homogeneous porosity and He concentration<sup>12,14</sup> on a laboratory scale, without the need for ion implantation facilities, which could be easily scaled up to an industrial process.

Another disadvantage of He-implanted foils is the reported high amounts of carbon and oxygen<sup>16,17</sup> that produce intense backgrounds. In implanted targets also, adequate choice of the host material is very important, and low-Z materials are preferred, as they will induce less beam scattering and thus less background. We will show how our bottom-up methodology is suitable for the preparation of self-supported amorphous silicon coatings, as thin-film solid He targets, that would allow scattering studies in forward geometry.

Here, the versatility of the methodology to produce a-Si:He coatings with different He contents is confirmed. The validation of our coatings as solid He targets takes place in two parts. On the first example, a self-supported coating is used as a proof of concept to illustrate the potential of our films to be used as a

solid He target in inverse kinematics studies with exotic nuclei beams. For this kind of experiments, targets must be self-supported, with an amount of He as high as possible in low thickness and a low c/He ratio, where c refers to contamination elements that could cause interferences in the spectra. The scattering of a <sup>6</sup>Li beam on this sample is studied for a fixed angle of 30°, illustrating its potential use in inverse kinematics studies with radioactive beams, for example <sup>11</sup>Li.

On the second example, the differential cross-section of the reaction <sup>4</sup>He(p,p)<sup>4</sup>He was determined at laboratory angles between 110 and 165° for proton energies between 0.6 and 3.0 MeV, comparing our results with available datasets. Different ion beam analysis (IBA) methods are based on the registration of elastically scattered particles or the products of nuclear reactions, and a reliable source of cross-section data is needed. In particular, proton elastic backscattering (p-EBS) has been established as a valuable analytical technique for the detection of light elements such as He, especially in materials research.<sup>22</sup> A strong signal enhancement, of 2–3 orders of magnitude, is achieved in p-EBS of light species in thin films relative to the corresponding Rutherford value. The sensitivity depends on whether the low-energy backscattered ion signal (in this case He) can be separated from the background signals of the host material or substrate. Depth resolution and sensitivity can be increased by increasing the incidence angle with respect to the normal of the target surface, and usually scattering angles between 150 and 175° are desirable for separating various scattered and reaction particles. However, because of the cross-section dependence on angle, the available data are valid only in the case of a scattering geometry very close to the geometry used in the cross-section measurements. Intensive research work can be found in the literature,<sup>20,21,23–28</sup> however, some discrepancies in reported cross-sections are related to the target nature and associated restrictions.<sup>20,21</sup> In this work, we present a comparison between our data and those reported in the literature by other authors for similar conditions and targets of different nature,<sup>20,21,23–28</sup> evidencing the use of our coatings as solid He targets.

The stability of the closed porous structure, in particular of He inside the pores over time (up to 2 years after deposition), and also after ion irradiation is demonstrated here.

## RESULTS AND DISCUSSION

### Characterization of Helium-Charged Silicon Coatings.

As mentioned in the Introduction section, one of the major requirements of thin films to be used as solid He targets is a high He concentration. Adequate choice of deposition parameters will determine the amount of He incorporated. From our previous works,<sup>12,15</sup> we observed that for the same deposition pressure condition, high rf power (of 300 W) resulted in a decrease in He incorporated into the coatings when compared to lower rf power (21 atom % for 300 W and 34 atom % for 150 W). In this work, the effect of helium



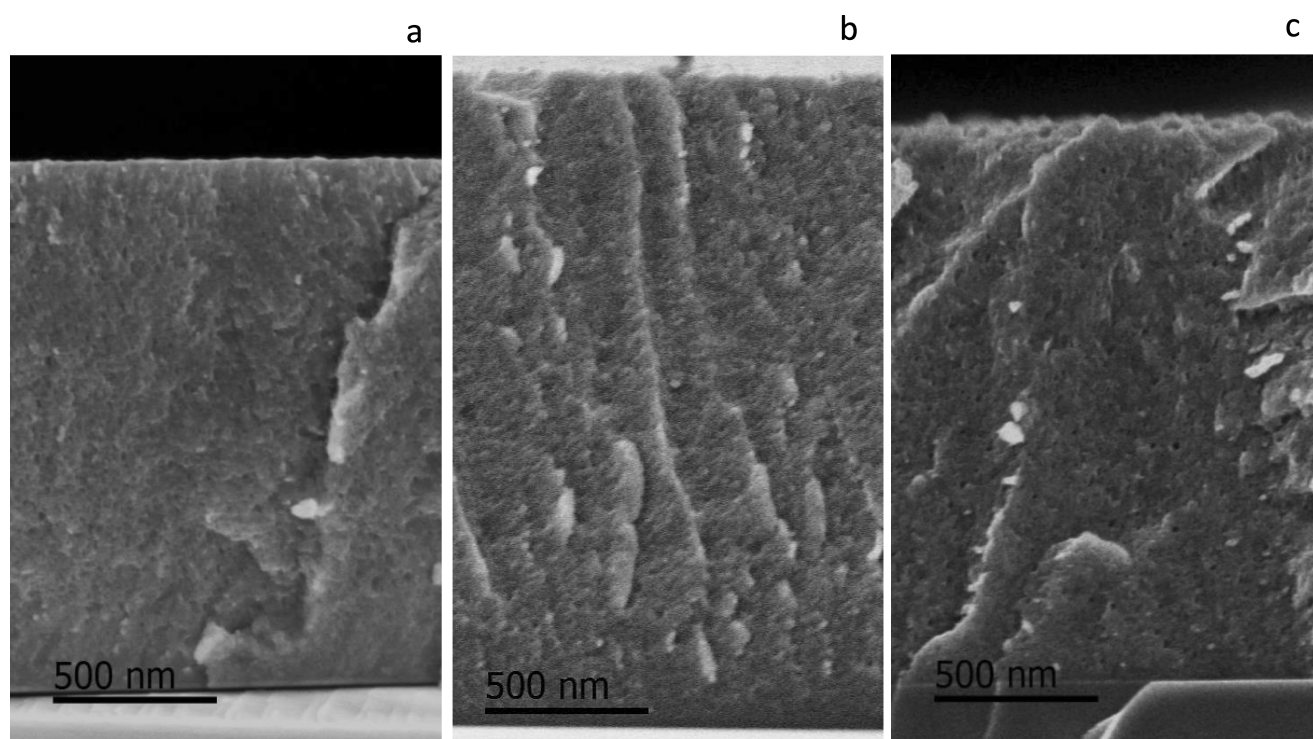


**Figure 1.** SEM cross-sectional views of samples: (a) a-Si:He\_LP, (b) a-Si:He\_MP, and (c) a-Si:He\_HP.

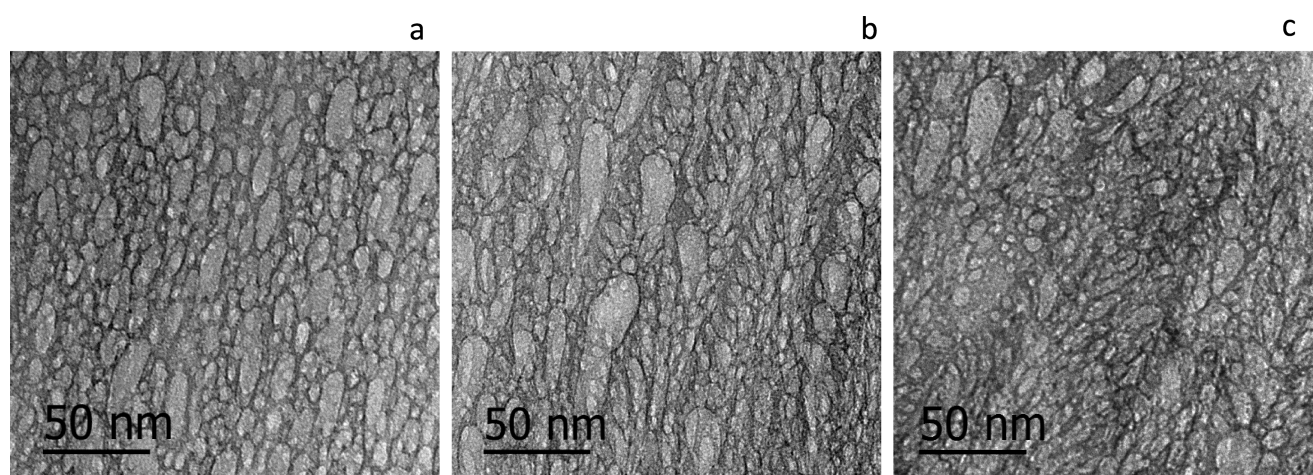


**Figure 2.** Details of porous structure by TEM cross-sectional views: (a) a-Si:He\_LP, (b) a-Si:He\_MP, and (c) a-Si:He\_HP.

deposition pressure is explored for the selected power condition allowing the highest He incorporation (i.e., 150 W).

Other authors<sup>29–31</sup> have also reported the effects of He partial pressure in mixtures of He + Ar in dc magnetron sputtering of metals on the He incorporation into the coatings. However, our approach explores the possibility of producing porous silicon coatings incorporating different helium amounts by rf magnetron sputtering at 150 W, using pure helium as the deposition gas; as summary, Table 1 presents the deposition conditions selected, and the labels of the coatings.

The morphology of the coatings deposited by magnetron sputtering at 150 W in rf, under 2.7, 4.9, and 9.0 Pa of He was first characterized by SEM-FEG cross-sectional images on coatings deposited on silicon substrates (see Figure 1). The coatings present a highly porous structure evenly distributed from the substrate to the surface, similar to the morphology

previously reported by us for coatings deposited under a single pressure condition.

The closed porous structure can be observed in detail in the transmission electron microscopy (TEM) images in Figure 2, where the pores in bright contrast have sizes between 2 and 50 nm. Figure 3 displays the pore size distribution corresponding to the major diameter of an ellipse (best fitted to each pore), for samples deposited under increasing He deposition pressure. The values were taken from around 100 pores per sample. At intermediate pressure, a significant increase in the number of pores with diameters between 10 and 20 nm is observed with respect to the low-pressure sample where the majority of pores have sizes around 10 nm. Under high-pressure conditions, a large number of very small pores (with major diameters below 10 nm) combined with bigger pores (up to 50 nm) is observed.

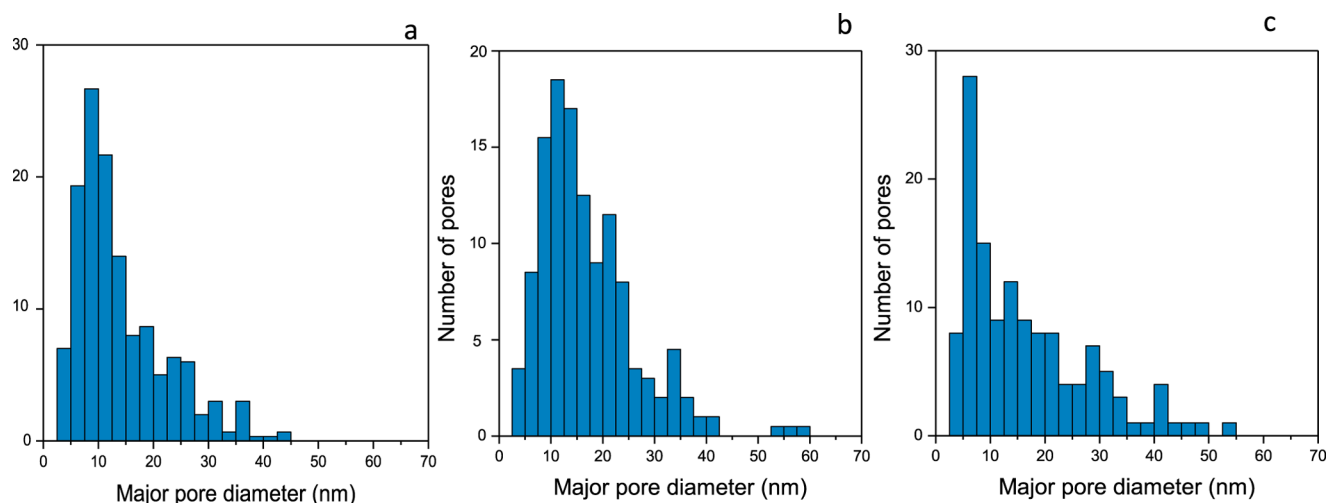


**Figure 3.** Pore size (major diameter of pore's best fitted ellipse) distribution from TEM cross-sectional images: (a) a-Si:He\_LP, (b) a-Si:He\_MP, and (c) a-Si:He\_HP.

The composition of the samples produced under increasing helium pressure was analyzed by p-EBS measurements, and the results of He/Si are displayed in Table 1. A significant decrease in the incorporated He amount is obtained as the deposition pressure increases. A large amount of He is incorporated when the coatings are prepared at 2.7 Pa (He/Si = 0.79), which decreases for a working pressure of 4.9 Pa to a He/Si atomic ratio of 0.49. To understand this result, we may refer to our previous paper in ref 15, where a relation between the pore radius and He inside the pores was found: for smaller pore sizes, higher He pressure and density inside the pores were observed. Notice that the sample presenting higher He incorporation is also the sample presenting smaller pores with a narrower pore size distribution. Therefore, in the case of the sample deposited at 9.0 Pa, a larger decrease in the He amount in the samples should be expected as bigger pores are observed; however, the large number of very small pores seems to compensate for this effect presenting a He/Si atomic ratio of 0.39.

As an example, the p-EBS spectrum of the sample deposited at a higher He pressure is presented in Figure 4. Our results in Table 1 demonstrate experimentally that it is possible to control the He incorporation into the silicon coatings by

controlling the deposition pressure in rf discharges using only He as the deposition gas. It is worth mentioning that the presence of contamination elements was below 2 atom % or negligible.

Apart from high He density, homogeneity versus depth is fundamental for the use of these coatings as solid He targets. As already mentioned, the coatings present high porosity from the substrate to the surface, presenting homogeneous composition as well, as can be observed in the spectrum in Figure 4. This is a typical spectrum of protons backscattered from the helium-containing porous samples. The peak of helium appears over the signal corresponding to the Si substrate. The observed increase in the Si signal and the small decrease in the He signal are related to variation of the cross-section with energy and not to any change in the concentration depth profile of these elements. A constant concentration for both elements has been used in the simulation.

Reproducibility of He incorporation and stability over time was also investigated. For that purpose, a coating deposited under the same conditions as those for coating a-Si:He\_MP was prepared using a shorter deposition time (in fact, several substrates were coated at the same time under these preparation conditions). Figure S1a presents the SEM cross-sectional view of this coating (called a-Si:He\_MP(bis)) showing its porosity, which can be observed in more detail in the TEM micrograph of Figure S1b. A similar pore structure to the one presented in Figure 2 is observed. Figure 5 shows characteristic p-EBS spectra of the as-prepared a-Si:He\_MP(bis) sample, which clearly shows a narrower He signal, as expected for this thinner sample.

To investigate the reproducibility and stability of the He incorporated over time, the composition of coatings (a-Si:He\_MP(bis)) deposited at the same time was measured by p-EBS few days and few months after its deposition and then 2 years later. No particular procedure was followed to store the samples (storage in ambient air). As can be appreciated in Figure 5, the spectra of the samples are very similar over time. Although in Figure 5 a small difference can be observed regarding the He signal for the sample measured after 2 years, the He/Si content remains constant within experimental error (He/Si atomic ratio of ~0.48). The small difference that can be observed is related to a small change in thickness observed in

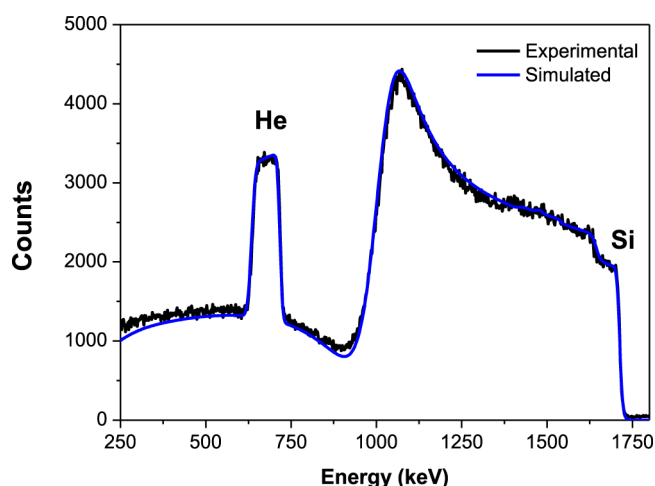


**Figure 4.** p-EBS spectrum of sample a-Si:He\_HP.



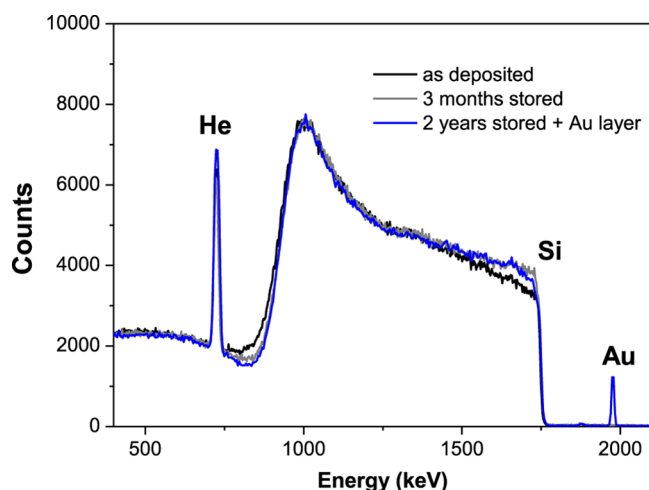


**Figure 5.** p-EBS spectra of sample a-Si:He\_MP(bis) over time.

the samples owing to their position in the sample holder. Nevertheless, it is important to emphasize that the He amount in the coating remains unaltered at least 2 years after deposition. This aspect is relevant for applications where He storage is of interest and therefore, for the fabrication of the He solid targets. It is relevant to comment that the spectrum of the sample stored for 2 years corresponds to the sample that will be used for the cross-section determination presenting an Au layer, as described in the [Experimental](#) (sample called Au/a-Si:He/Si sample). Further results on the stability of He in the coatings after irradiation are presented in section [a-Si:He Thin-Film Solid Target for Experiments of Elastic Scattering with Stable Beams](#).

**Scattering of Stable  $^6\text{Li}$  in a-Si:He Thin Film as a Test for Studies of Nuclear Properties of Radioactive Nuclei by Inverse Kinematics.** Due to the low ion current achieved by the radioactive beams compared with stable ones, the total amount of He in a solid target must be as high as possible in the smallest thickness to minimize the energy loss and the angular straggling produced in the sample. In the previous section, the ability to produce thin films with high He amount homogeneously distributed throughout the film thickness was demonstrated. However, to fulfill the requirements of a solid

He target for inverse kinematics studies, and to realize experiments in forward geometry, self-supported thin films are desired. To explore the possibility of producing a self-supported a-Si:He film to be used as a solid He target, some considerations must be taken into account regarding not only the required high He amount, but a reasonable thickness must also be selected to have a compromise between low thickness and still to ensure easy handling and mechanical stability during measurements. In this case, as described in the [Experimental](#), a coating was deposited on a NaCl substrate under similar deposition conditions to those of sample a-Si:He\_MP, presenting the highest deposition rate, with a thickness of 2300 nm. After deposition, the a-Si:He coating was floated off in distilled water and transferred to a holder with an aperture of 10 mm for measurements. [Figure 6a](#) presents a SEM cross-sectional view of the self-supported porous a-Si:He coating to be used as a target (a-Si:He\_MP(self-supp.)). It is possible to appreciate that the coating has a similar morphology to those presented by the coatings deposited on silicon substrates. In [Figure 6b](#), the porous structure of the target is shown in more detail by TEM cross-section. The photographs in [Figure 6c](#) show a piece of the self-supported thin film on a tweezer and the film already transferred to the holder for measurements.

The He content in the coating was first checked by p-EBS. [Figure 7](#) presents the obtained spectrum for 2.0 MeV proton energy and at detection angle  $165^\circ$ . The coating is composed of 29 atom % He and 66 atom % Si, and in this case also, a small oxygen signal is observed (5 atom % O), most probably due to residual oxygen in the deposition chamber or insufficient sputtering target cleaning before deposition. [Table 2](#) compares the He incorporation into our a-Si:He\_MP self-supported thin film and into other targets, reported in the literature prepared by ion implantation. We can see in [Table 2](#) that the total amount of He in our sample is higher than the quantity obtained by other groups for implanted samples, also proposed as He targets for inverse kinematics experiments. Our He/M ( $M = \text{Si}$  in this work or  $\text{Al}$  in the case of other authors) ratio is double the value obtained by Vanderbist et al.<sup>19</sup> (0.25) and is much higher than that obtained by Raabe et al.<sup>16</sup> and Ujic et al.<sup>32</sup> Relative to the impurity content, in our case only oxygen, the O/He ratio is lower than 0.22, which is the lowest value reported in these works.<sup>19</sup>

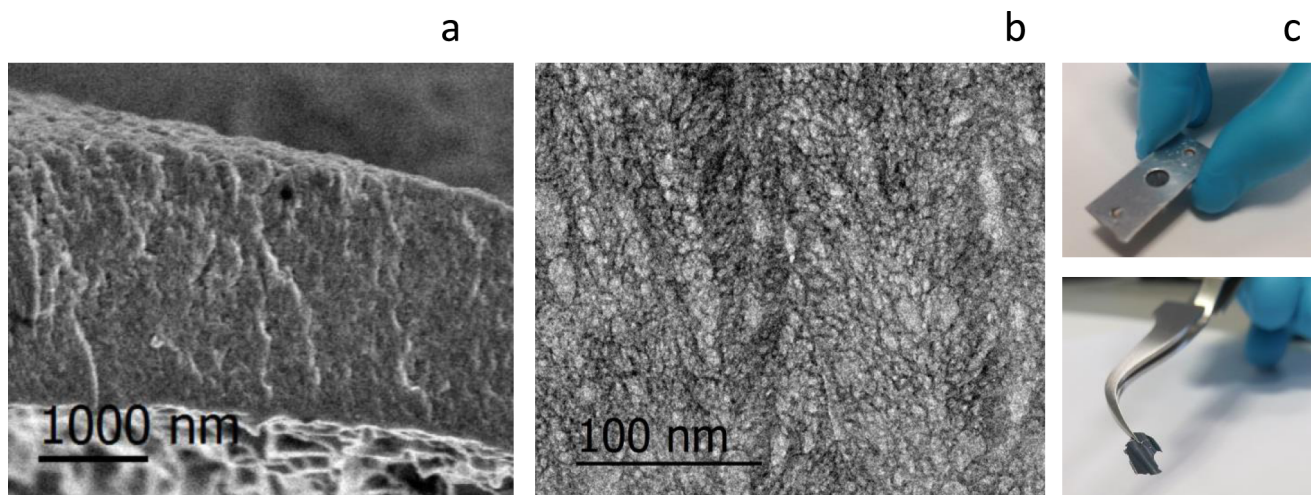


**Figure 6.** Self-supported a-Si:He thin film: (a) SEM and (b) TEM cross-sectional views. (c) Down: photograph of the self-supported thin film, up: thin film mounted on the holder for measurements.

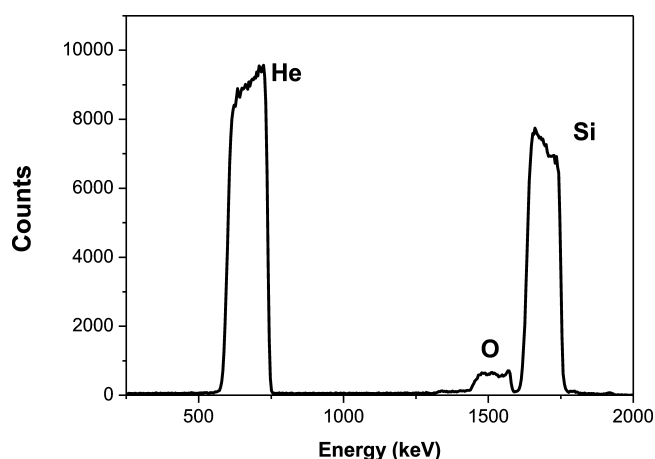


Figure 7. p-EBS spectrum of the a-Si:He\_MP(self-supp.) target.

To show the potential of the self-supported a-Si:He coatings prepared by our methodology, as a target for experiments of scattering of exotic beams, a preliminary measurement using a similar forward geometry and a stable beam of  ${}^6\text{Li}$  was performed. For the  ${}^6\text{Li}^{2+}$  forward scattering experiment, the self-supported coating was placed on a holder, as shown in Figure 6c, and bombarded with  ${}^6\text{Li}^{2+}$  ions at 6 MeV. The experimental setup is schematized in Figure 8a, and the scattering spectrum measured at  $30^\circ$  is presented in Figure 8b. Even if the acquisition system and, consequently, the spectrum can be improved, this preliminary experiment is used here as proof of concept to demonstrate the fact that the Li ions can traverse the sample, and the energies of the dispersed Li, or recoiled ions, are the ones predicted by kinematics. Nevertheless, the results presented here represent a novel approach for the production of self-supported coatings as solid He targets by magnetron sputtering. Further experiments with stable beams are being proposed to improve the quality of the spectra, and these preliminary studies serve as a verification test of our self-supported samples for measurements with radioactive beams.

**a-Si:He Thin-Film Solid Target for Experiments of Elastic Scattering with Stable Beams.** The excitation functions for the direct scattering process  $\text{He}(p,p)\text{He}$  between  $110$  and  $165^\circ$  are presented in Figure 9 (obtained values are also presented in Table S1), as obtained from experiments with our Au/a-Si:He/Si solid He target. Data are compared to the reported results in the literature at similar angles, using He targets of different nature.<sup>20,21,23–28</sup> The scattering angles in the cited works are slightly different from those measured in our work; nevertheless, the data presented in Figure 9 are compared with published graphs at a similar scattering angle. In general, our cross-section curves agree well, both in shape

and in absolute values, with the data available in the literature. As expected, the cross-section maxima are systematically lower for smaller scattering angles.<sup>20</sup>

For  $165$ ,  $150$ , and  $135^\circ$ , the curves increase swiftly from  $0.6$  until a broad maximum is reached around an energy of  $2.2$  MeV, and after this maximum, cross-sections decrease with increasing energy. Attending to the value of the maximum resonance, we observe that data at  $165^\circ$  differ by less than 2% from the data presented by Lu<sup>21</sup> at this angle, and by less than 5% in the absolute value between the values obtained by Miller<sup>24</sup> at  $164^\circ$  and the ones presented by Kraus<sup>25</sup> at  $163^\circ$ . The data obtained at  $150^\circ$  are 2% higher than the values presented by Cai<sup>27</sup> at  $151^\circ$  and 10% higher than those by Kraus<sup>25</sup> at  $150^\circ$ . At  $135^\circ$ , our values are 10% higher than the data obtained by Barnard<sup>26</sup> and Kraus<sup>25</sup> at  $135^\circ$  but differ by less than 2% from the values by Freier<sup>23</sup> at  $140^\circ$ .

In the case of the data obtained at  $110^\circ$ , between  $0.6$  and  $0.8$  MeV, a decrease in the cross-section values is observed with the increase in energy, followed by a similar behavior of the previous curves for higher energies. At the cross-section maxima, the difference is less than 1% compared to data from Miller<sup>24</sup> at  $112^\circ$ .

It is worth pointing out again the different nature of the targets used, and that the differences found could be due to instabilities inherent to the nature of the He target used in the previous measurements as already reported by other authors.<sup>20</sup> Even with differences up to 10%, these results point out that our porous silicon coatings are good candidates to be used as solid He targets.

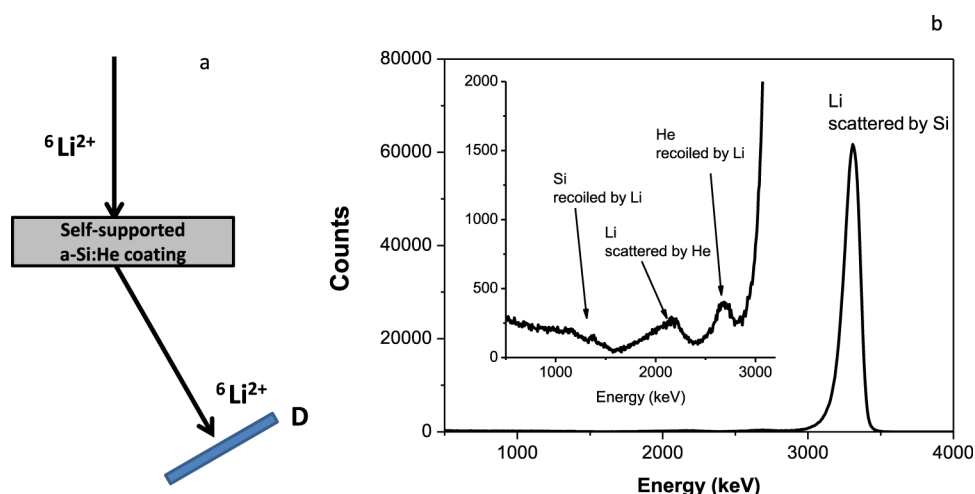
Furthermore, it is important to notice the stability of samples after irradiation. In Figure 10, we can see the spectra of the sample before and after the experimental measurements performed with the proton ion beams. The sample was submitted to a total irradiation fluence of  $5 \times 10^{17}$  particles/ $\text{cm}^2$ , with a dose rate of  $5 \times 10^{12}$  particles/( $\text{cm}^2 \text{ s}$ ), and no significant differences in the He content were observed, demonstrating once again the high stability of the target coatings.

## EXPERIMENTAL SECTION

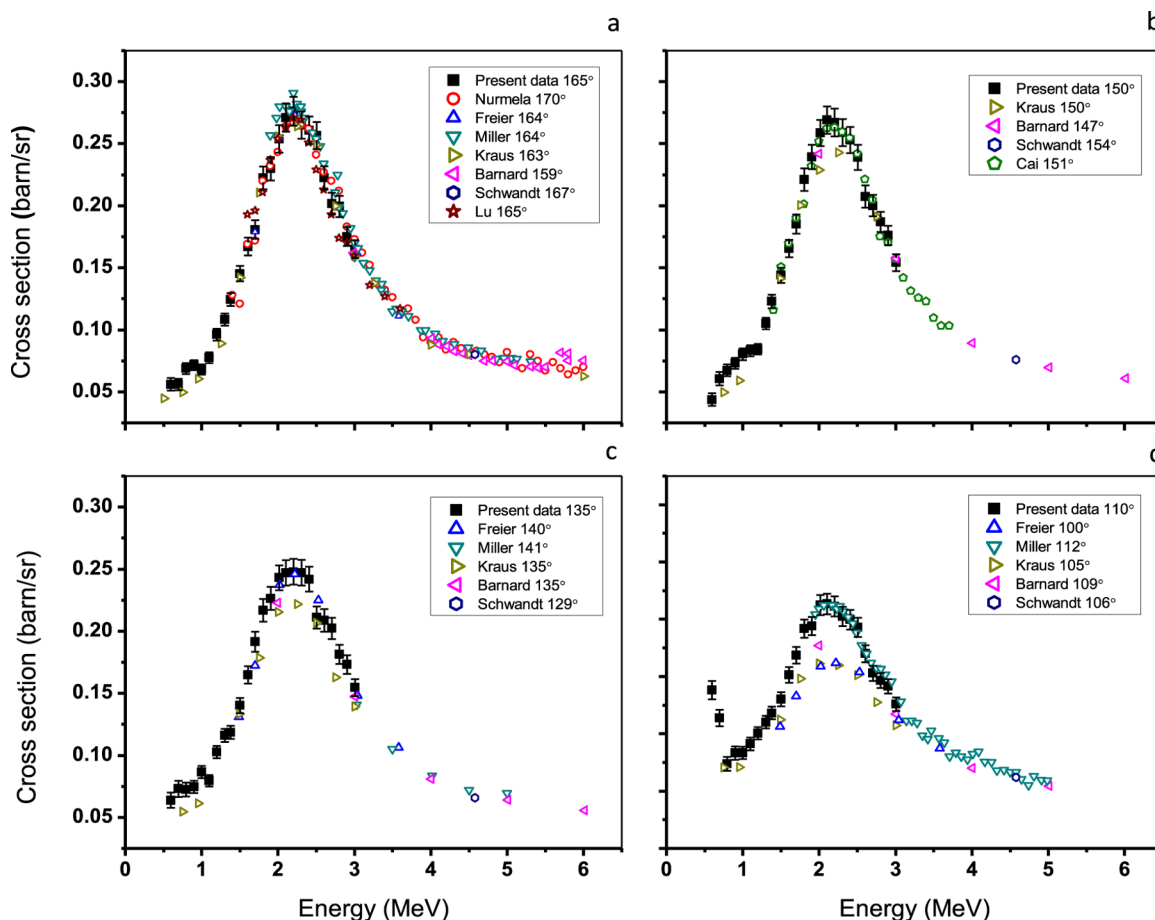
**Preparation and Characterization of Helium-Charged Silicon Coatings.** In this work, the effect of helium deposition pressure on the formation of closed porosity and He incorporation was investigated. A 2 inch magnetron gun (ION'X from Thin Film Consulting, Germany) equipped with a pure Si target (99.999% purity; KurtJ Lesker), placed at 5 cm from the sample holder, was used. The He deposition pressure was changed from  $2.7$  to  $9.0$  Pa for a deposition power of  $150$  W in rf mode. Table 1 shows the deposition conditions employed in the preparation and the labels of the coatings. The coatings were deposited on silicon substrates (100) of  $525 \mu\text{m}$

Table 2. Comparison of He Incorporation vs Contaminants by Magnetron Sputtering (Sample a-Si:He\_MP(Self-Supp.) in Present Work) and He Implantation<sup>16,19,36</sup>

	magnetron sputtering		ion implantation	
	present work	Vanderbist et al. <sup>19</sup>	Raabe et al. <sup>16</sup>	Ujic et al. <sup>32</sup>
metal ( $\times 10^{15}$ atoms/ $\text{cm}^2$ )	(Si) $9250 \pm 463$	(Al) 1100	(Al) 4200	(Al) 1200
He ( $\times 10^{15}$ atoms/ $\text{cm}^2$ )	$4060 \pm 203$	275	270	130
O ( $\times 10^{15}$ atoms/ $\text{cm}^2$ )	$700 \pm 35$	60	100	not mentioned
O/He	0.17	0.22	0.37	not mentioned
He/M	0.44	0.25	0.06	0.11



**Figure 8.** Experimental geometry of the forward scattering experiment (a) and resulting spectrum (b); the inset shows in more detail the spectrum between 500 and 3200 keV.



**Figure 9.** Obtained He(p,p)He elastic scattering cross-section at scattering angles of 165° (a), 150° (b), 135° (c), and 110° (d) as a function of proton energy at our laboratory (with the Au/a-Si:He/Si sample) in comparison to earlier data published at similar angles.

thickness. For investigating the reproducibility of the deposition procedure, several substrates were coated simultaneously.

The composition of the coatings was evaluated at the 3 MV NEC 9SDH-2 tandem accelerator of the National Center for Accelerators (CNA, Seville, Spain) by p-EBS spectrometry, following the method described in ref 22, using a beam of 2.0 MeV and a passivated implanted planar silicon (PIPS) detector set at 165°, and using the evaluated (SigmaCalc) cross-sections

obtained from the IBANDL database, IAEA base.<sup>33,34</sup> The p-EBS spectra were analyzed with the SIMNRA software.<sup>35</sup> The absolute energy calibration of the tandem accelerator was determined utilizing resonances of 991.86 keV for reaction  $^{27}\text{Al}(p,\gamma)^{28}\text{Si}$  and 2409 keV for reaction  $^{24}\text{Mg}(p,p'\gamma)^{24}\text{Mg}$ , and RBS with a thin Au target for energies in the range 4.5–6.2 MeV. After calibration, the beam energy had a precision better than  $\pm 5$  keV and energy spread of around 1 keV. The



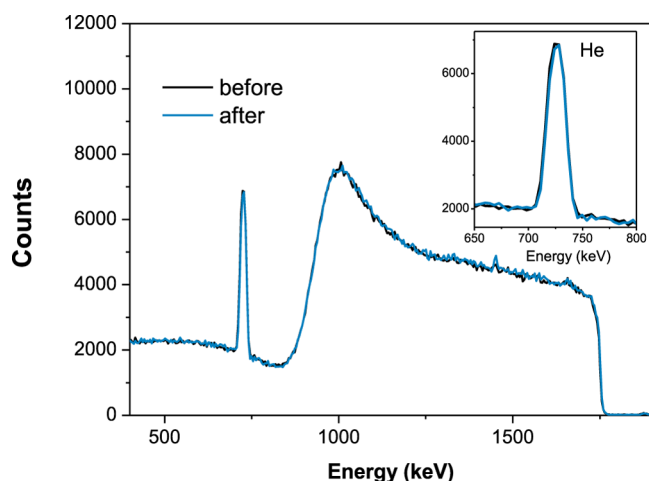


**Figure 10.** Spectra of sample a-Si:He\_MP(bis) before and after the experimental measurements performed with the proton ion beam. The sample was submitted to a total irradiation fluence of  $5 \times 10^{17}$  particles/cm<sup>2</sup>. The inset shows in detail the He signal.

uncertainty associated with the determination of the absolute concentration of the elements was less than 5%.

The thickness and morphology of the samples were examined by scanning electron microscopy (HITACHI S-4800 SEM-FEG). The samples deposited on silicon substrates were cleaved and observed without metallization in cross-sectional views at 1–2 kV.

The microstructure of the porous films was investigated using the TEM at the Laboratory of Nanoscopies and Spectroscopies (LANE-ICMS; Sevilla, Spain), a Philips CM200, and a Tecnai G2 F30 operating at 200 and 300 kV, respectively. The cross-sectional TEM samples were prepared from the coatings deposited on silicon, by mechanical polishing and dimple grinding, followed by Ar<sup>+</sup> ion milling to electron transparency. The pore distribution was evaluated from the TEM micrographs by binarizing them and then using the “Analyze Particle” function of the ImageJ software.<sup>36</sup>

**Self-Supported a-Si:He Thin-Film Solid Target for Exotic Nuclei Experiments.** The feasibility of the use of the self-supported coating as a solid target in inverse kinematics experiments with exotic nuclei was investigated. Samples were prepared under similar conditions to those used for sample a-Si:He\_MP and characterized as indicated in the previous section. To obtain self-supported films, the coatings were grown on NaCl substrates and then floated off in distilled water and dried in air.

Elastic scattering of <sup>6</sup>Li by the target as a proof of concept to future studies of the <sup>4</sup>He(<sup>6</sup>Li, <sup>6</sup>Li)<sup>4</sup>He cross-section was performed at the 3 MV tandem accelerator of the CNA using a beam of 6.0 MeV and a PIPS detector set at 30°.

**EBS Spectrometry. Experimental Conditions and Apparatus.** To demonstrate the potential use of the porous silicon coatings as solid helium targets in nuclear reactions, EBS spectrometry was employed to determine the elastic scattering cross-sections of protons from helium.

For this purpose, an Au overlayer of  $1.1 \times 10^{16}$  atoms/cm<sup>2</sup> was deposited by evaporation over a porous Si film (prepared at MP conditions) to prepare an Au/a-Si:He/Si target for the cross-section measurements. The Au film is important as it is used as an internal ion dose reference and can also prevent the surface of the silicon coating from further oxidation. The

thickness of this layer was chosen so that the amount of Au is low enough to avoid an important energy loss or spread in the target and high enough to obtain an important signal in the p-EBS spectra. The helium amount in the coating was checked by p-EBS, as described above in this Experimental.

The 3 MV tandem accelerator at CNA provided the incident proton beams used for the cross-section measurements, in the energy range from 0.6 to 3.0 MeV at 100 keV steps.

A PIPS detector with a thickness of 500 μm was placed at the laboratory backward angles between 110 and 165° and subtended a solid angle of  $5 \times 10^{-3}$  sr, set by a defining circular aperture of 50 mm<sup>2</sup>. The angular resolution of the detector was thus 4.5°. The energy resolution of the detection system was typically 10 keV for protons. The beam was confined to a diameter of 1.0 mm before bombarding the target, and the beam current was limited to less than 8 nA. The beam current was kept sufficiently low to ensure that pulse pile-up through the detector system deadtime was minimized and to avoid possible loss of He during the experiment. The accumulated charge per energy interval was 10 μC measured using an Ortec 439 digital current integrator. The Au/a-Si:He/Si target was very stable under bombardment by 8 nA proton beams and no helium losses were observed during 10 μC runs.

**Proton-Helium Cross-Section Determination.** The elastic scattering differential cross-section of proton-helium in the laboratory coordinates, using the Au/a-Si:He/Si sample as the target, was calculated from

$$\frac{d\sigma}{dE_{\text{He}}}(E, \theta) = \frac{d\sigma}{dE_{\text{Au,Ruth}}}(E_0, \theta) \cdot \left( \frac{A_{\text{He}}}{A_{\text{Au}}} \right) \cdot \left( \frac{Nt_{\text{Au}}}{Nt_{\text{He}}} \right) \quad (1)$$

where  $\frac{d\sigma}{dE_{\text{Au,Ruth}}}(E_0, \theta)$  is the calculated Rutherford differential scattering cross-section for protons on Au.  $E = E_0 - \Delta E_{\text{Au}} - \frac{1}{2}\Delta E_{\text{Si}}$  is the incident proton energy, and  $\Delta E_{\text{Au}}$  and  $\Delta E_{\text{Si}}$  are the energy loss of protons in the Au and Si films, respectively. The signal peak area ratio  $A_{\text{He}}/A_{\text{Au}}$  was determined from the measured spectrum. The ratio  $(Nt)_{\text{Au}}/(Nt)_{\text{He}}$  ( $N$  = atom density,  $t$  = layer thickness) was determined by using the areal density value for  $(Nt)_{\text{He}}$  and  $(Nt)_{\text{Au}}$  from the above-mentioned p-EBS spectra of the sample. All Rutherford scattering cross-sections used here were corrected for electron screening effects.<sup>37</sup>

The accuracy of the proton differential elastic scattering cross-sections measured here is limited by the uncertainties in all parameters used in eq 1. The statistical uncertainties of  $A_{\text{Au}}$  and  $A_{\text{He}}$  come from the determination of Au and He peak areas and the background subtraction, and they are typically 1–2% for Au and 1–9% for He (depending on the energy used in the measurement). These values could be improved using a different experimental setup, as for example an  $E - \Delta E$  telescope detection system that avoids the uncertainties from the background subtraction. The uncertainties from measuring the areal density  $(Nt)_{\text{Au}}$  and  $(Nt)_{\text{He}}$  are less than 3%. As the energy straggling is negligible, its effect on the accuracy of cross-section measurements has not been accounted for. Thus, the total uncertainty associated with the measured cross-section is between 4 and 10%.

The stability of He content throughout the experiment was checked. p-EBS measurements, using 2.0 MeV, at both the beginning and the end of the experiments were performed.

## CONCLUSIONS

In this work, we have demonstrated the possibility of controlling the He amount in amorphous Si:He coatings with closed porosity by controlling the deposition pressure. The coatings deposited by the presented methodology are good candidates to be used as solid He targets as a high He amount is incorporated into the film homogeneously distributed throughout the film thickness. The versatility of magnetron sputtering and the reproducibility of the results make this a very promising methodology for extended target production. Moreover, the coatings proved to be stable in time, at least 2 years after deposition and after irradiation.

A strategy to produce self-supported a-Si:He coatings with high He amount is presented here for the first time. Preliminary results in forward geometry using a  $^6\text{Li}$  beam are used here as a proof of concept to show that the self-supported coatings can be used as alternative He solid targets for experiments with radioactive beams.

The validation of the a-Si:He porous coatings as solid He targets is further demonstrated by the determination of the differential cross-section for the elastic scattering of proton-helium in the energy range from 0.6 to 3.0 MeV at laboratory angles from 110 to 165°. In general, our results are consistent, both in shape and absolute values, with the data available in the literature for He targets of different nature (gas, implanted, and coatings).

## ASSOCIATED CONTENT

### Supporting Information

The Supporting Information is available free of charge on the ACS Publications website at DOI: 10.1021/acsomega.6b00270.

(a) SEM and (b) TEM cross-sectional views of sample a-Si:He\_MP(bis) (Figure S1); obtained He(p,p)He differential elastic scattering cross-section at scattering angles of 165, 150, 135, and 110° as a function of proton energy in the laboratory frame (Table S1) (PDF)

## AUTHOR INFORMATION

### Corresponding Authors

\*E-mail: godinho@icmse.csic.es (V.G.).

\*E-mail: fferrer@us.es (F.J.F.).

\*E-mail: asuncion@icmse.csic.es (A.F.).

### ORCID

Vanda Godinho: 0000-0003-1829-6674

Asunción Fernández: 0000-0002-7487-7054

### Notes

The authors declare no competing financial interest.

## ACKNOWLEDGMENTS

This work was supported by the Spanish Ministry MINECO (projects FPA2013-47327-C2-1-R and MAT2015-69035-REDC), the CSIC (PIE 201460E018) and the EU 7FP (Project AI-NanoFunc CT-REGPOT-2011-285895) and the OpenAIRE FP7 Post-grant open access pilot program for open access publication funding. The authors also acknowledge the Laboratory for Nanoscopies and Spectroscopies (LANE) for the TEM facilities.

## REFERENCES

- (1) Tanyeli, I.; Marot, L.; van de Sanden, M. C. M.; De Temmerman, G. Nanostructuring of Iron Surfaces by Low-Energy Helium Ions. *ACS Appl. Mater. Interfaces* **2014**, *6*, 3462–3468.
- (2) de Respinis, M.; De Temmerman, G.; Tanyeli, I.; van de Sanden, M. C. M.; Doerner, R. P.; Baldwin, M. J.; van de Krol, R. Efficient Plasma Route to Nanostructure Materials: Case Study on the Use of m-WO<sub>3</sub> for Solar Water Splitting. *ACS Appl. Mater. Interfaces* **2013**, *5*, 7621–7625.
- (3) Kajita, S.; Yoshida, N.; Ohno, N.; Hirahata, Y.; Yoshihara, R. Helium plasma irradiation on single crystal tungsten and undersized atom doped tungsten alloys. *Phys. Scr.* **2014**, *89*, No. 025602.
- (4) Iyyakkunnel, S.; Marot, L.; Eren, B.; Steiner, R.; Moser, L.; Mathys, D.; Dueggelin, M.; Chapon, P.; Meyer, E. Morphological Changes of Tungsten Surfaces by Low-Flux Helium Plasma Treatment and Helium Incorporation via Magnetron Sputtering. *ACS Appl. Mater. Interfaces* **2014**, *6*, 11609–11616.
- (5) Ullmaier, H. The influence of helium on the bulk properties of fusion reactor structural materials. *Nucl. Fusion* **1984**, *24*, 1039.
- (6) Gai, X.; Smith, R.; Kenny, S. D. Inert gas bubbles in bcc Fe. *J. Nucl. Mater.* **2016**, *470*, 84–89.
- (7) Lucas, A. A. Helium in metals. *Physica B+C* **1984**, *127*, 225–239.
- (8) Petersen, G. A.; Myers, S. M.; Follstaedt, D. M. Gettering of transition metals by cavities in silicon formed by helium ion implantation. *Nucl. Instrum. Methods Phys. Res., Sect. B* **1997**, *127–128*, 301–306.
- (9) Kouadri-boudjelthia, E. A.; Ntsoenzok, E.; Benoit, R.; Regula, G.; Etienne, H.; Michel, T.; Ashok, S. Plasma immersion ion implantation: A viable candidate for low cost purification of mc-Si by nanocavities? *Nucl. Instrum. Methods Phys. Res., Sect. B* **2016**, *366*, 150–154.
- (10) Kajita, S.; Yoshida, T.; Kitaoka, D.; Etoh, R.; Yajima, M.; Ohno, N.; Yoshida, H.; Yoshida, N.; Terao, Y. Helium plasma implantation on metals: Nanostructure formation and visible-light photocatalytic response. *J. Appl. Phys.* **2013**, *113*, No. 134301.
- (11) Godinho, V.; Fernandez, A. Procedimiento de obtención de recubrimientos mediante pulverización catódica y recubrimiento obtenible mediante dicho procedimiento. P200930085, 2009.
- (12) Godinho, V.; Caballero-Hernández, J.; Jamon, D.; Rojas, T. C.; Schierholz, R.; García-López, J.; Ferrer, F. J.; Fernández, A. A new bottom-up methodology to produce silicon layers with a closed porosity nanostructure and reduced refractive index. *Nanotechnology* **2013**, *24*, No. 275604.
- (13) Lacroix, B.; Godinho, V.; Fernández, A. Nitrogen Nanobubbles in a-SiOxNy Coatings: Evaluation of Its Physical Properties and Chemical Bonding State by Spatially Resolved Electron Energy-Loss Spectroscopy. *J. Phys. Chem. C* **2016**, *120*, 5651–5658.
- (14) Caballero-Hernandez, J.; Godinho, V.; Lacroix, B.; Jimenez de Haro, M. C.; Jamon, D.; Fernandez, A. Fabrication of Optical Multi layer Devices from Porous Silicon Coatings with Closed Porosity by Magnetron Sputtering. *ACS Appl. Mater. Interfaces* **2015**, *7*, 13889–13897.
- (15) Schierholz, R.; Lacroix, B.; Godinho, V.; Caballero-Hernandez, J.; Duchamp, M.; Fernandez, A. STEM-EELS analysis reveals stable highdensity He in nanopores of amorphous silicon coatings deposited by magnetron sputtering. *Nanotechnology* **2015**, *26*, No. 075703.
- (16) Raabe, R.; Andreyev, A.; Huyse, M.; Piechaczek, A.; Van Duppen, P.; Weissman, L.; Woehr, A.; Angulo, C.; Cherubini, S.; Musumarra, A.; Baye, D.; Descouvemont, P.; Davinson, T.; Di Pietro, A.; Laird, A. M.; Ostrowski, A.; Shotton, A.; Galanina, L. I.; Zelenskaya, N. S. 2n-transfer contribution in the He-4(He-6,He-6)He-4 cross section at E-c.m. = 11.6 MeV. *Phys. Rev. C* **2003**, *67*, No. 044602.
- (17) Blackmon, J. C.; Angulo, C.; Shotton, A. C. Experimental approaches to nuclear reactions involved in explosive stellar binaries. *Nucl. Phys. A* **2006**, *777*, 531–549.
- (18) Weissman, L.; Raabe, R.; Huyse, M.; Koops, G.; Pattyn, H.; Terwagne, G.; Van Duppen, P. An implanted 4He target for experiments with radioactive beams. *Nucl. Instrum. Methods Phys. Res., Sect. B* **2000**, *170*, 266–275.

- (19) Vanderbist, F.; Angulo, C.; Couder, M.; El Masri, Y.; Leleux, P.; Loiselet, M.; Tabacaru, G. Realization and analysis of He-implanted foils for the measurement of (alpha, gamma) reaction cross-sections in nuclear astrophysics. *Nucl. Instrum. Methods Phys. Res., Sect. B* **2002**, *197*, 165–171.
- (20) Nurmela, A.; Rauhala, E.; Raisanen, J. Elastic scattering cross sections for the p + He system in the energy region of 1.4–24 MeV. *J. Appl. Phys.* **1997**, *82*, 1983–1988.
- (21) Lu, Y. F.; Shi, L. Q.; He, Z. J.; Zhang, L.; Zhang, B.; Hutton, R. Elastic scattering cross-section of proton from helium at the laboratory angle of 165 degrees. *Nucl. Instrum. Methods Phys. Res., Sect. B* **2009**, *267*, 760–762.
- (22) Ferrer, F. J.; Alcaire, M.; Caballero-Hernandez, J.; Garcia-Garcia, F. J.; Gil-Rostra, J.; Terriza, A.; Godinho, V.; Garcia-Lopez, J.; Barranco, A.; Fernandez-Camacho, A. Simultaneous quantification of light elements in thin films deposited on Si substrates using proton EBS (Elastic Backscattering Spectroscopy). *Nucl. Instrum. Methods Phys. Res., Sect. B* **2014**, *332*, 449–453.
- (23) Freier, G.; Lampi, E.; Sleator, W.; Williams, J. H. Angular distribution of 1-mev TO 3.5-mev protons scattered by He-4. *Phys. Rev.* **1949**, *75*, 1345–1347.
- (24) Miller, P. D.; Phillips, G. C. Scattering of Protons from Helium and Level Parameters in Li<sup>3</sup>. *Phys. Rev.* **1958**, *112*, 2043–2047.
- (25) Kraus, L.; Linck, I. Study of P3-2 and P1-2 levels of He-5 and Li-5 nuclei via He-4 + N and he-4 + P scattering. *Nucl. Phys. A* **1974**, *224*, 45–60.
- (26) Barnard, A. C. L.; Weil, J. L.; Jones, C. M. Elastic scattering of 2–11 MeV protons by He4. *Nucl. Phys.* **1964**, *50*, 604–620.
- (27) Cai, T.; Li, J. Q.; He, Z. J.; Wang, X. F.; Shi, L. Q. Measurements of the elastic scattering cross sections for proton on T, He-4. *Nucl. Instrum. Methods Phys. Res., Sect. B* **2010**, *268*, 3373–3376.
- (28) Schwandt, P.; Clegg, T. B.; Haeberli, W. Polarization measurements and phase shifts for p-4He scattering between 3 and 18 MeV. *Nucl. Phys. A* **1971**, *163*, 432–448.
- (29) Zheng, H.; Liu, S.; Yu, H. B.; Wang, L. B.; Liu, C. Z.; Shi, L. Q. Introduction of helium into metals by magnetron sputtering deposition method. *Mater. Lett.* **2005**, *59*, 1071–1075.
- (30) Jia, J.-p.; Shi, L.-q.; Lai, X.-c.; Wang, Q.-f. Preparation of Al thin films charged with helium by DC magnetron sputtering. *Nucl. Instrum. Methods Phys. Res., Sect. B* **2007**, *263*, 446–450.
- (31) Shi, L.; Liu, C.; Xu, S.; Zhou, Z. Y. Helium-charged titanium films deposited by direct current magnetron sputtering. *Thin Solid Films* **2005**, *479*, 52–58.
- (32) Ujic, P.; Lagoyannis, A.; Mertzimekis, T. J.; de Oliveira Santos, F.; Harissopulos, S.; Demetriou, P.; Perrot, L.; Stodel, C.; Saint-Laurent, M. G.; Kamalou, O.; Lefebvre-Schuhl, A.; Spyrou, A.; Amthor, M. A.; Grevy, S.; Caceres, L.; Koivisto, H.; Laitinen, M.; Uusitalo, J.; Julin, R. Alpha-particle capture reactions in inverse kinematics relevant to p-process nucleosynthesis. In *Frontiers in Nuclear Structure, Astrophysics, and Reactions*; Demetriou, P., Julin, R., Harissopulos, S. V., Eds.; AIP, 2011; pp 321–325.
- (33) [www-nds.iaea.org/ibandl](http://www-nds.iaea.org/ibandl).
- (34) Gurbich, A. F. SigmaCalc recent development and present status of the evaluated cross-sections for IBA. *Nucl. Instrum. Methods Phys. Res., Sect. B* **2016**, *371*, 27–32.
- (35) Eckstein, W.; Mayer, M. Rutherford backscattering from layered structures beyond the single scattering model. *Nucl. Instrum. Methods Phys. Res., Sect. B* **1999**, *153*, 337–344.
- (36) Rasband, W. S. U. S., *ImageJ*; National Institutes of Health: Bethesda, MD, 1997–2012. [imagej.nih.gov/ij/](http://imagej.nih.gov/ij/).
- (37) Andersen, H. H.; Besenbacher, F.; Loftager, P.; Moller, W. Large-angle scattering of light-ions in the weakly screened Rutherford region. *Phys. Rev. A* **1980**, *21*, 1891–1901.